

RESEARCH ARTICLE

10.1002/2018JE005558

Constraining the Potential Liquid Water Environment at Gale Crater, Mars

Key Points:

- Measured surface environmental conditions at Gale crater are not favorable to brine formation via deliquescence of calcium perchlorate
- Liquids may have formed in the shallow subsurface of low thermal inertia units within MSL-traversed terrains
- MSL may best find liquids in the subsurface of units with thermal inertia less than or equal to $175 \text{ J m}^{-2} \text{ K}^{-1} \text{ s}^{-1/2}$ and albedo > 0.25 around $\text{Ls } 100^\circ$

Supporting Information:

- Supporting Information S1
- Data Set S1
- Data Set S2
- Data Set S3

Correspondence to:

E. G. Rivera-Valentín, ervalentin@usra.edu

Citation:

Rivera-Valentín, E. G., Gough, R. V., Chevrier, V. F., Primm, K. M., Martínez, G. M., & Tolbert, M. (2018). Constraining the potential liquid water environment at Gale crater, Mars. *Journal of Geophysical Research: Planets*, 123, 1156–1167. <https://doi.org/10.1002/2018JE005558>

Received 26 JAN 2018

Accepted 26 MAR 2018

Accepted article online 31 MAR 2018

Published online 11 MAY 2018

Edgard G. Rivera-Valentín^{1,2}, Raina V. Gough^{3,4}, Vincent F. Chevrier⁵, Katherine M. Primm^{3,4}, German M. Martínez⁶, and Margaret Tolbert^{3,4}

¹Arecibo Observatory, Universities Space Research Association, Arecibo, PR, USA, ²Lunar and Planetary Institute, Universities Space Research Association, Houston, TX, USA, ³Cooperative Institute for Research in Environmental Sciences, University of Colorado Boulder, Boulder, CO, USA, ⁴Department of Chemistry and Biochemistry, University of Colorado Boulder, Boulder, CO, USA, ⁵Arkansas Center for Space and Planetary Sciences, University of Arkansas, Fayetteville, AR, USA, ⁶Department of Climate and Space Sciences and Engineering, University of Michigan, Ann Arbor, MI, USA

Abstract The Mars Science Laboratory (MSL) Rover Environmental Monitoring Station (REMS) has now made continuous in situ meteorological measurements for several Martian years at Gale crater, Mars. Of importance in the search for liquid formation are REMS' measurements of ground temperature and in-air measurements of temperature and relative humidity, which is with respect to ice. Such data can constrain the surface and subsurface stability of brines. Here we use updated calibrations to REMS data and consistent relative humidity comparisons (i.e., with respect to liquid versus with respect to ice) to investigate the potential formation of surface and subsurface liquids throughout MSL's traverse. We specifically study the potential for the deliquescence of calcium perchlorate. Our data analysis suggests that surface brine formation is not favored within the first 1648 sols as there are only two times (sols 1232 and 1311) when humidity-temperature conditions were within error consistent with a liquid phase. On the other hand, modeling of the subsurface environment would support brine production in the shallow subsurface. Indeed, we find that the shallow subsurface for terrains with low thermal inertia ($\Gamma \lesssim 300 \text{ J m}^{-2} \text{ K}^{-1} \text{ s}^{-1/2}$) may be occasionally favorable to brine formation through deliquescence. Terrains with $\Gamma \lesssim 175 \text{ J m}^{-2} \text{ K}^{-1} \text{ s}^{-1/2}$ and albedos of $\gtrsim 0.25$ are the most apt to subsurface brine formation. Should brines form, they would occur around $\text{Ls } 100^\circ$. Their predicted properties would not meet the Special nor Uncertain Region requirements, as such they would not be potential habitable environments to life as we know it.

Plain Language Summary The Mars Science Laboratory (MSL) has now made continuous measurements of the local weather at Gale crater, Mars. Such measurements can help guide our search for the formation of liquid water on present-day Mars. Specifically, when the right temperature and humidity conditions are met, certain salts can take in water vapor from the atmosphere to produce liquids. Here we use data from MSL along with experimental results on the stability of a Mars-relevant salt to search for time periods when liquids could potentially form at the surface. Additionally, we use simulations and MSL data to understand the potential to form such liquids in the subsurface. Our results suggest that surface formation of liquids is unlikely throughout MSL's travels; however, the shallow subsurface may experience conditions that would allow for liquid formation. Not much liquid would form, though, and the properties of these liquids would not permit life as we know it to persist.

1. Introduction

At large spatial scales, the present Martian atmospheric conditions preclude the formation of pure liquid water at the surface (Haberle et al., 2001). The formation of transient brines, though, has long been hypothesized since the discovery that the Martian surface is composed of a few weight percent salt (Brass, 1980; Clark, 1978; Ingersoll, 1970). Perchlorate (ClO_4^-) salts have now been identified in situ by the Phoenix lander (Hecht et al., 2009), potentially at the two Viking sites (Navarro-Gonzalez et al., 2010), by the Mars Science Laboratory (MSL) Curiosity rover (Leshin et al., 2013; Ming et al., 2014), possibly in the form of hydrated calcium perchlorate ($\text{Ca}(\text{ClO}_4)_2 \cdot n\text{H}_2\text{O}$; Glavin et al., 2013) and from orbit at sites with recurring slope lineae (RSL) activity (Ojha et al., 2015). Such salts are interesting because of their ability to transition from a solid crystalline salt

into an aqueous solution given the appropriate temperature and relative humidity (i.e., deliquescence; Fischer et al., 2014; Gough et al., 2011, 2014; Nikolakakos & Whiteway, 2017; Nuding et al., 2014; Zorzano et al., 2009). Calcium perchlorate can produce brines above temperatures of 198 K (Marion et al., 2010; Pestova et al., 2005), the lowest known eutectic temperature for pure component brines of Mars-relevant salts. Calcium perchlorate has been shown to deliquesce at a relative humidity with respect to (w.r.t.) liquid of $RH_l \sim 50\%$ and not effloresce (i.e., transition from aqueous to solid) until a much lower $RH_l \sim 3\%$ (Nuding et al., 2014), making it ideal for liquid production on present-day Mars. Furthermore, liquid formation through deliquescence of calcium perchlorate has been shown to allow for a viable environment for microorganisms under Mars-like conditions (Nuding et al., 2017), suggesting a potentially astrobiologically interesting process.

Indeed, the search for liquid water on present-day Mars has largely been driven by astrobiology, and also as a potential trigger mechanism or fluid for mass wasting events, such as gullies (Johnsson et al., 2014; Malin & Edgett, 2003; Massé et al., 2016), slope streaks (Kreslavsky & Head, 2009; Sullivan et al., 2001), dark dune spots (Kereszturi & Rivera-Valentín, 2012; Kereszturi et al., 2010), and RSL (Chevrier & Rivera-Valentín, 2012; Dundas et al., 2017; McEwen et al., 2011, 2013). Potential visible confirmation of liquid water, though, has only come in the form of droplets on the lander legs of Phoenix (Rennó et al., 2009). At Phoenix, the presence of liquid water was also inferred by the heterogeneous distribution of salts within the regolith (Cull et al., 2010), which could potentially have been relocated by thin films of solutions, and by the measured changes in regolith dielectric signatures during nighttime (Stillman & Grimm, 2011). Such interpretations of liquids at the Phoenix landing site have further been supported by experimental results that suggest a role for deliquescence (Chevrier et al., 2009; Fischer et al., 2016; Nuding et al., 2014).

Liquid production through deliquescence, though, has been suggested to be constrained to a select few regions on Mars (Kossacki & Markiewicz, 2014; Martínez & Renno, 2013). However, recently, surface meteorological conditions derived from the Rover Environmental Monitoring Station (REMS) suggested favorable conditions for brine production through deliquescence of calcium perchlorate at the surface and shallow subsurface of Gale crater (Martin-Torres et al., 2015). REMS data, though, have undergone several calibrations (Martínez et al., 2017), the last of which was on June 2015. The latest calibrations have led to drier conditions, but, more importantly, previous investigations have compared relative humidity w.r.t. ice (RH_i) as measured by REMS to a phase diagram w.r.t. liquid water (e.g., Gough et al., 2016; Martin-Torres et al., 2015; Martínez et al., 2017; Pal & Kereszturi, 2017; Rummel et al., 2014). Indeed, MSL REMS measures air relative humidity at a height of 1.6 m using a capacitance-based hygrometer calibrated to RH_l (Harri et al., 2014). Under the low temperatures measured at Gale crater (~ 180 K; Hamilton et al., 2014) the difference between RH_l and RH_i can be on the order of 50% because of the significant difference between the respective saturation vapor pressures. This difference could drastically alter interpretation of potential brine formation events through deliquescence. Here we use consistent relative humidity comparisons when analyzing MSL REMS temperature and relative humidity data in search of favorable conditions on the surface for brine formation via deliquescence of calcium perchlorate. Additionally, we simulate the subsurface environment at Gale crater to investigate the potential for deliquescence of calcium perchlorate in order to provide guidance to future operation strategies for the rover and elucidate the role of deliquescence in the near-surface Martian water cycle at equatorial regions.

2. Data Analysis

The MSL Curiosity rover landed on the floor of Gale crater (4.7°S , 137°E) on 5 August 2012 and, as of January 2018, has been operating for more than 1900 sols (almost three Martian years). Among its 10 science instruments (Grotzinger et al., 2012), the REMS is a suite of sensors designed to assess the environmental conditions along Curiosity's traverse (Gomez-Elvira et al., 2012; Hamilton et al., 2014; Harri et al., 2014). The REMS instrument includes six sensors that measure ground and air temperature, wind velocity and relative humidity w.r.t. to ice at 1.6-m height on the rover mast and atmospheric pressure and ultraviolet radiation at about 1-m height on the rover deck. The REMS nominal strategy for data acquisition consists of 5 min of measurements at 1 Hz every Mars hour, with interspersed full hour sample periods at 1 Hz to cover every time of the sol over a period of a few sols.

In this work, we focus on REMS measurements performed by the relative humidity sensor (RHS) and ground temperature sensor (GTS) during the first 1648 sols. The RHS consists of three polymeric sensors that measure the air relative humidity with respect to ice (RH_{i_a}) and a sensor that measures the temperature of the air (T_a)

entering the RHS (Harri et al., 2014). The uncertainty in RH_{i_a} is $\pm 20\%$ for $T_a < 203$ K, $\pm 10\%$ for 203 K $\leq T_a \leq 243$ K, and $\pm 2\%$ for $T_a > 243$ K, while for T_a the uncertainty is 0.2 K. Among the full set of RHS measurements, we only consider those taken during the first 4 s after the RHS has been turned on after at least ~ 5 min of inactivity. After 4 s, the RHS is affected by heating produced by the sensor itself, which increases its temperature by up to 1.5 K. Thus, the local RH_{i_a} measured by the sensor is closest to the actual value of the atmosphere only during the first few seconds of operation. Reliable RH_{i_a} values include measurements taken during the nominal and the so-called high-resolution interval mode, which consists of alternately switching the sensor on and off at periodic intervals to minimize heating and is only used on selected 1- to 2-hr observation blocks (see Figure 13 in Martínez et al., 2017). Since during these 4 s RH_{i_a} values stay stable, this strategy typically results in 24 hourly values of RH_{i_a} and T_a under nominal measuring strategy.

The GTS measures the intensity of infrared radiation emitted by the ground in the bandwidths 8–14, 15.5–19, and 14.5–15.5 μm , from which the surface brightness can be derived (Sebastián et al., 2010). It uses three thermopiles pointed 26° downward from the plane of the rover deck with a field of view of 60° horizontally and 40° vertically, covering a ground area of about 100 m^2 depending on the angle between the surface and sensor. For details on random and systematic uncertainties on GTS measurements, see Hamilton et al. (2014) and the supporting information in Martínez et al. (2016). Among the full set of GTS measurements, we only consider here those with the highest confidence possible, specifically those with the ASIC power supply in range, the highest recalibration quality, and with no shadows in the GTS field of view. By averaging these GTS measurements over 5-min long intervals centered at simultaneous RHS measurements of the highest confidence and by imposing that at least 60 GTS measurements must be averaged to reduce noise, we produce high-quality hourly values of ground temperature (T_g) simultaneous to RH_{i_a} .

Using simultaneous hourly values of the highest possible confidence of RH_{i_a} and T_g , ground relative humidity was inferred assuming that water vapor pressure is constant throughout the 1.6-m air column such that $RH_{i_g} = RH_{i_a} [p_{\text{sat}_i}(T_a)/p_{\text{sat}_i}(T_g)]$, where p_{sat_i} is the saturation vapor pressure for ice (Feistel & Wagner, 2007). Water vapor pressure, which can be inferred by $P_{\text{H}_2\text{O}} = RH_{i_a} \times p_{\text{sat}_i}(T_a)$, is not expected to be constant from ground to a height of 1.6 m. Indeed, the gradient between ground and air will vary throughout the day as the planetary boundary layer (PBL) height changes (Savijärvi et al., 2016; Zent et al., 1993). During daytime there does not exist a strong gradient between surface and a height of 1.6 m because the PBL height approaches the scale height allowing for vigorous mixing of water vapor; however, at nighttime, the PBL is thin and gradients in water vapor between near surface and air form (Zent et al., 1993). In the absence of a reliable way to extract water vapor pressure at the ground, though, we make this simplifying assumption.

Propagating error from REMS measurements, we found that most low RH_{i_g} have large errors that do not preclude the unphysical possibility of $RH_{i_g} < 0\%$; therefore, these values were not included in our analysis. This filter on the data results in a loss of information during the warmest periods at Gale crater, which approached temperatures of ~ 290 K as measured by GTS. Additionally, some REMS measurements suggest $RH_{i_g} > 100\%$, even up to 500%, which is unrealistic. We note, though, that super saturation w.r.t. ice has been shown to occur at high altitudes within the Martian atmosphere (Maltagliati et al., 2011), and ice supersaturation of $RH_i \sim 170\%$ is often observed in Earth's atmosphere (Jensen et al., 2013). For completeness, we present data in both RH_i and RH_{i_g} space up to saturation within the relevant phase space.

2.1. Surface Deliquescence of Calcium Perchlorate

Typically, the phase diagram of brines is presented with respect to temperature and water activity (a_w) or concentration in weight percent, which also relates to a_w (e.g., Chevrier et al., 2009; Gough et al., 2011, 2014; Hanley et al., 2012; Nuding et al., 2014). Under equilibrium conditions, $a_w = RH_i/100$ (Murphy & Koop, 2005), and so in situ humidity data can be directly compared with the phase diagram of salts after some modification. Fundamentally, though, a liquid forms when the partial pressure of water is above the partial pressure at the eutectic point and simultaneously the temperature is above the eutectic temperature; therefore, the most direct way to search for liquid production would be to compare in situ inferred $P_{\text{H}_2\text{O}}$ and temperature with a phase diagram in the same terms. However, thus far in situ humidity measurements on Mars have been measurements of RH_i . Inferring $P_{\text{H}_2\text{O}}$ from RH_i and temperature, and propagating the errors in both measurements, typically leads to large errors in $P_{\text{H}_2\text{O}}$ because of the exponential dependency in p_{sat_i} . Here in order to search for environmental conditions appropriate for the deliquescence of calcium perchlorate, we compared REMS data to the phase diagram of $\text{Ca}(\text{ClO}_4)_2$ in RH_i (Figure 1a) and in RH_{i_g} phase space (Figure 1b) to be consistent

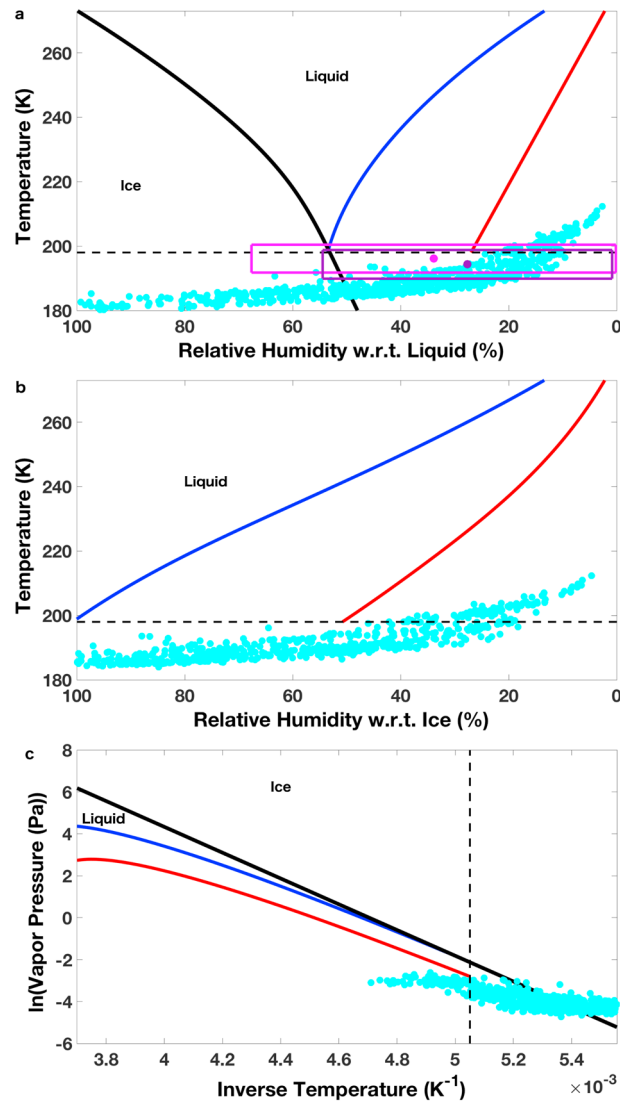


Figure 1. Mars Science Laboratory Rover Environmental Monitoring Station (REMS) measured ground temperature and inferred ground relative humidity on the phase diagram of calcium perchlorate in relative humidity (a) w.r.t. liquid, (b) w.r.t. ice phase space, and (c) in $1/T_g$ versus $\ln(P_{H_2O})$ space. The blue and red lines are the deliquescence relative humidity and efflorescence relative humidity respectively from Nuding et al. (2014), while REMS data are in cyan circles. The black dashed line is the eutectic temperature of calcium perchlorate brine, 198 K. In (a) the black solid line is the ice line, where $RH_i = 100\%$ in RH_i phase space, while in (b) it is at the left-hand plot axis, and in (c) the black solid line is the saturation vapor pressure of ice as a function of temperature. In (a) measurements for sol 1232 (magenta) and 1311 (purple) are shown with 2-sigma error in temperature and 1-sigma in relative humidity, illustrated by the, respectively, colored box. Because error in relative humidity is large, even at the 1-sigma, we do not investigate the 2-sigma effect.

with previous results and to more confidently search for humidity-temperature conditions that could permit liquid formation. We also compare with respect to P_{H_2O} (Figure 1c) for completeness.

REMS inferred RH_g was converted to relative humidity w.r.t. liquid by $RH_g = RH_i \left[\frac{p_{sat_i}(T_a)}{p_{sat_l}(T_g)} \right]$, where p_{sat_l} is the saturation vapor pressure of liquid water, equation (10) from Murphy and Koop (2005). Modeled deliquescence relative humidity (DRH) is presented in blue in Figure 1 (Nuding et al., 2014). Thermodynamically, efflorescence relative humidity is indistinguishable from DRH; however, experimental work has shown that calcium perchlorate, like many salts, undergoes a hysteresis effect, efflorescing at much lower relative humidity conditions. Here we use fits to experimental data from Nuding et al. (2014) to extrapolate the efflorescence relative humidity behavior of $Ca(ClO_4)_2$ as a function of temperature (red in Figure 1). In Figure 1a, the ice line (i.e., $RH_i = 100\%$ in RH_i phase space) is presented as a black solid line.

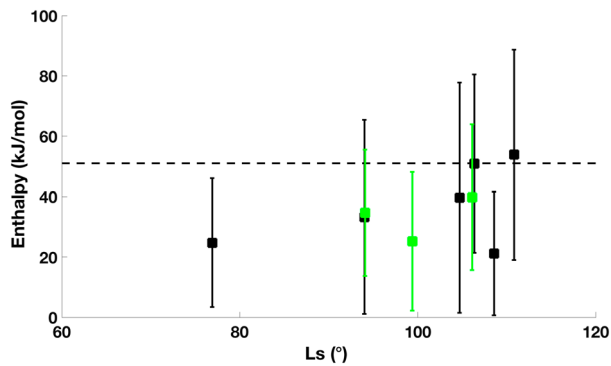


Figure 2. Derived nonzero enthalpies over 5 sols from time spans of 3 a.m. to 6 a.m. (black squares) and 6 a.m. to 9 a.m. (green squares) with error bars to 90% confidence as a function of Ls. The black dashed line is the enthalpy of sublimation of water ice (50.9 kJ/mol).

Accounting for updated REMS data calibrations and comparing relative humidity values in consistent phase space, we found that no measured environmental condition would permit for the deliquescence of calcium perchlorate at the surface. Accounting for error, we found that to the 1-sigma level for T_g and RH_{l_g} deliquescence is still unfavored; however, to the 2-sigma level for T_g , 1-sigma for RH_{l_g} , there are two points on sols 1232 and 1311, Ls 99° and Ls 137°, respectively, that could be within the liquid phase. These values, delineated in Figure 1a, occurred while the rover was near active sand dunes (Vasavada et al., 2017) during the early morning and late evening. Accounting for 2-sigma level error in T_g would still preclude the formation of liquids via deliquescence of other hygroscopic salts, such as magnesium perchlorate, the next most stable Mars-relevant single component brine, which has a eutectic temperature of 205 K and eutectic concentration of $a_w = 0.55$ (Gough et al., 2011).

Our conclusion that surface humidity-temperature conditions are not favorable to liquid production is valid only for single-salt brines. Multicomponent brines, which would be expected on Mars, would have lower DRH

compared to each individual salt. Such multicomponent solutions would also have lower eutectic temperatures. Indeed, the DRH of binary mixtures was found to be lower than that of the least deliquescent salt in the system (Gough et al., 2014). Therefore, multicomponent brines may be more stable on the Martian surface.

2.2. Surface Enthalpy Changes

Active near-surface processes, such as sublimation, condensation, hydration state changes, and deliquescence, result in enthalpy changes (ΔH) that can be inferred from water vapor pressure and temperature provided equilibrium conditions are assumed (e.g., Rivera-Valentín & Chevrier, 2015; Zent et al., 2010). The inferred ΔH is the sum of all active processes during the studied time span, and so this procedure can provide information on the dominant ongoing near-surface processes. Thus, following the methods of Rivera-Valentín and Chevrier (2015), we searched for surface enthalpic changes during nighttime as a potential signature of phase changes, specifically within 3-hr time spans from midnight to 3 a.m., 3 a.m. to 6 a.m., 6 a.m. to 9 a.m., 6 p.m. to 9 p.m., and 9 p.m. to midnight.

Vapor pressure curves were constructed using the REMS-measured surface temperatures along with the inferred water vapor pressure at 1.6 m. Data were binned over 5 sols for each studied time span to increase the statistics. Following the Clausius-Clapeyron relation for transitions between gas and a condensed phase,

$$\ln(P_{\text{H}_2\text{O}}) = -\frac{\Delta H}{R} \left(\frac{1}{T_g} \right) + c, \quad (1)$$

such that the slope in $1/T_g$ versus $\ln(P_{\text{H}_2\text{O}})$ space is linear and related to enthalpy by $\Delta H = -\beta R$ (Murphy & Koop, 2005; Rivera-Valentín & Chevrier, 2015), where β is the slope, R is the ideal gas constant, and c is a constant. Here we used a weighted least squares fit method to derive β . The weighted least squares fit slope, which accounts for error following the York method (York et al., 2004) of each MSL measurement in T_g and inferred $P_{\text{H}_2\text{O}}$, was found to 90% confidence. To test for statistical significance of β , we test for the null hypothesis (i.e., that $1/T_g$ contributes no information for the prediction of $\ln(P_{\text{H}_2\text{O}})$); therefore, only nonzero slopes within error, and so nonzero ΔH , are accepted.

We found only nine significant (i.e., nonzero) enthalpic changes, all of which occurred during the early morning (six values during 3 a.m. to 6 a.m. and three values from 6 a.m. to 9 a.m.) primarily around Ls 100°. Inferred values with associated error, including propagation from measurement error, are shown in Figure 2, where colors delineate time span, as a function of Ls. Cumulatively, the derived values have a weighted average of $\Delta H = 33 \pm 20$ kJ/mol. Derived enthalpic changes were generally within error of the enthalpy of H_2O sublimation (50.9 kJ/mol), but the range of values does not preclude other processes such as adsorption/desorption, which has been suggested to be active within Gale crater (Savijärvi et al., 2016) or deliquescence (Jia et al., 2018). Of note, a nonzero-derived enthalpy on Ls 99° (sol 1232) could support liquid formation as indicated from the analysis in section 2.1 for sol 1232 after including 2-sigma error; however, no corresponding statistically significant ΔH was found for sol 1311. Derived values, though, agree with the hour

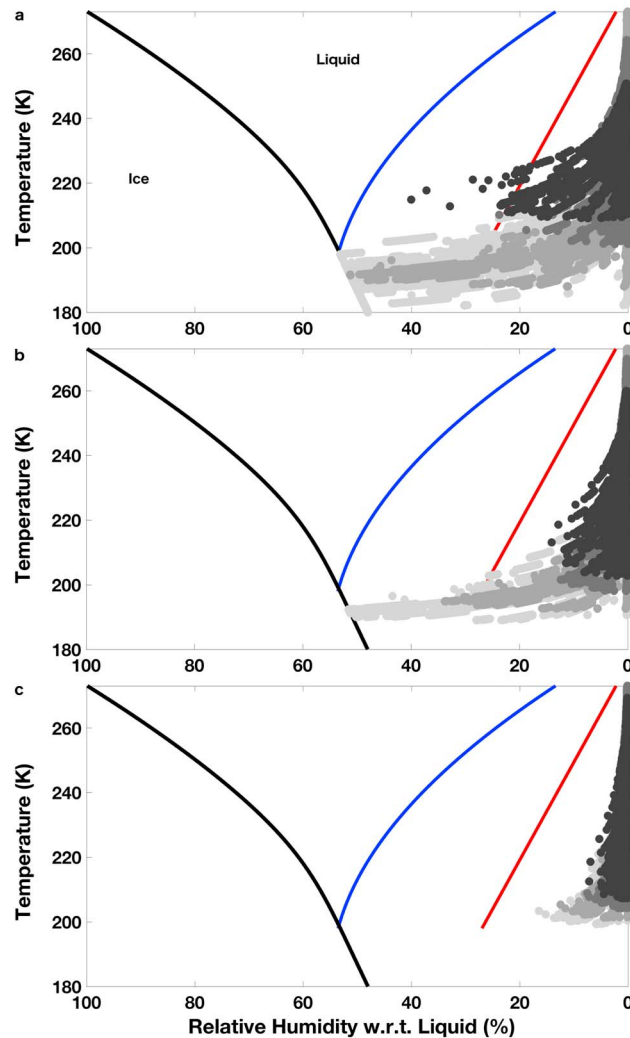


Figure 3. Simulated subsurface conditions in temperature and relative humidity w.r.t. to liquid phase space for likely terrains throughout Mars Science Laboratory's traverse, where (a) is $\Gamma = 180 \text{ J m}^{-2} \text{ K}^{-1} \text{ s}^{-1/2}$, $A = 0.11$, (b) $\Gamma = 350 \text{ J m}^{-2} \text{ K}^{-1} \text{ s}^{-1/2}$, $A = 0.2$, and (c) $\Gamma = 550 \text{ J m}^{-2} \text{ K}^{-1} \text{ s}^{-1/2}$, $A = 0.15$, as the low, typical, and high thermal inertia units traversed by the rover. Simulated hourly conditions for one Martian year are in gray-scaled circles, where from lightest to darkest are results for depth of 1, 2, 4, and 6 cm. Line colors follow from Figure 1.

(4 a.m. to 6 a.m.) and Ls range during which frost formation was likely within Gale crater (Martínez et al., 2016); therefore, derived enthalpic changes may support frost/sublimation as an active water vapor sink/source within Gale crater.

3. Subsurface Modeling

MSL has traversed various terrain types, which have included both low and high thermal inertia terrains that have deviated from the typical values found at the landing ellipse ($\Gamma \sim 350 \text{ J m}^{-2} \text{ K}^{-1} \text{ s}^{-1/2}$; Christensen et al., 2001; Putzig et al., 2005). Reported thermal inertia values in the first 1337 sols have ranged from $170 \text{ J m}^{-2} \text{ K}^{-1} \text{ s}^{-1/2}$ to $600 \text{ J m}^{-2} \text{ K}^{-1} \text{ s}^{-1/2}$, and albedo values have typically been $0.1 \leq A \leq 0.3$ (Martínez et al., 2014, 2016; Rodríguez Colon & Rivera-Valentín, 2016; Vasavada et al., 2017). Via a fully coupled heat and mass transfer model, we searched for potential subsurface liquid formation throughout one Martian year at locations the rover has traversed. Additionally, we explored liquid formation for various combinations of regolith thermal properties in order to better inform future MSL operational strategies and elucidate the potential for subsurface brine formation at equatorial regions on Mars using Gale crater as a proxy.

3.1. Methods

Subsurface temperatures were simulated by solving the 1-D thermal diffusion equation via a finite element procedure (Chevrier & Rivera-Valentin, 2012; Kereszturi & Rivera-Valentin, 2012; Nuding et al., 2014; Rivera-Valentin et al., 2011) with a vertical resolution of 0.01 m. The time step required for stable solutions is dependent on the thermal inertia of the regolith column and the vertical resolution; values used here ranged from 180 to 370 s. The surface boundary condition is radiative and includes direct illumination, along with scattering and thermal emission atmospheric components such that the incident heat flux is given by

$$Q_i = (1 - A) \frac{S_0}{r^2} [\psi \cos(\zeta) + (1 - \psi) f_{\text{scat}} + \epsilon \cos(\theta - \phi) f_{\text{atm}}], \quad (2)$$

where S_0 is the solar flux at 1 AU, r is the instantaneous Sun-Mars distance in AU, ζ is the solar zenith angle, ψ is the transmission coefficient, f_{scat} and f_{atm} are the fractional amounts of the relevant flux reaching the surface, ϵ is atmospheric thermal emissivity, and θ and ϕ are the solar declination and latitude, respectively (Aharonson & Schorghofer, 2006; Applebaum & Flood, 1989; Pollack et al., 1990; Schmidt et al., 2009). As applied by Blackburn et al. (2009), ψ is a polynomial fit to data from Pollack et al. (1990) as presented in Rapp (2008). By Schmidt et al. (2009), $f_{\text{scat}} = 0.02$, $f_{\text{atm}} = 0.04$, and $\epsilon = 0.9$. A flat surface is assumed, and so slope effects on thermal insolation were not accounted for (e.g., Aharonson & Schorghofer, 2006). Note that such simulations provide spatially and temporally averaged temperatures. Actual values may vary due to differences in regolith physical properties with depth and local geometry; however, the code has been validated against the Phoenix lander (Rivera-Valentin & Chevrier, 2015) and MSL (Rodriguez Colon & Rivera-Valentin, 2016) measurements and was further validated here.

Water vapor diffusion through regolith, which has been shown to be approximately Fickian (Clifford & Hillel, 1986) and undergo diffusion advection (Ulrich, 2009), follows

$$J_{DA} = \frac{\varphi}{\tau\mu} \left(D_{\text{H}_2\text{O}/\text{CO}_2} \frac{P}{RT} \frac{dy}{dz} + J_{DA} \right), \quad (3)$$

where $D_{\text{H}_2\text{O}/\text{CO}_2}$ is the diffusivity of water vapor through CO_2 gas, $\varphi = 0.5$ (Zent et al., 2010), and $\tau = 2$ (Hudson & Aharonson, 2008; Sizemore & Mellon, 2008) are the porosity and tortuosity, respectively, μ is the ratio between the molecular weights of H_2O and CO_2 , P is air pressure, and γ is the water vapor mixing ratio. The diffusivity of water vapor through CO_2 gas was modeled as temperature dependent following

$$D_{\text{H}_2\text{O}/\text{CO}_2} = 1.3875 \times 10^{-5} \left(\frac{T}{273.15} \right)^{\frac{3}{2}} \left(\frac{1}{P} \right), \quad (4)$$

where T is temperature and here P is specifically in bar (Chevrier & Altheide, 2008), which gives nominal values on the order of $10^{-4} \text{ m}^2 \text{ s}^{-1}$ (Bryson et al., 2008; Chevrier et al., 2007; Hudson et al., 2007; Schorghofer & Aharonson, 2005). Fits to REMS-derived water vapor pressure define the water vapor just above the regolith. Then, at the surface-atmosphere interface, a mass conservation boundary condition is applied, thereby coupling the REMS data to the model. Perturbative processes to simple diffusion, such as adsorption/desorption and frost formation, are not included.

Temperature was simulated to 4 m, beyond three times the annual skin depth (~ 1 m), which allows for accurate modeling of temperature variations with depth and time while mass transfer to a depth of 1 m. Simulations were run for several Martian years and considered converged when the temperature with depth profile for two separate consecutive runs at the vernal equinox ($L_s = 0^\circ$) were < 1 K different. We specifically tested the thermal inertia and albedo combinations for various terrains as found by Vasavada et al. (2017). Simulated surface temperatures and relative humidities were compared with surface-derived REMS values. For each terrain traversed by MSL, the code had on average an error of ± 5 K in temperature and $\pm 7\%$ in relative humidity with respect to REMS values and so was within error of MSL measurements.

3.2. Results

In Figure 3, subsurface environmental conditions at varying depths are plotted in the calcium perchlorate phase diagram with respect to RH_i for the low (3a), typical (3b), and maximum (3c) thermal inertia cases from Vasavada et al. (2017). Because simulations do not account for perturbative processes to water vapor diffusion, the maximum RH_i is set to saturation with respect to ice. For low thermal inertia terrain, we find that

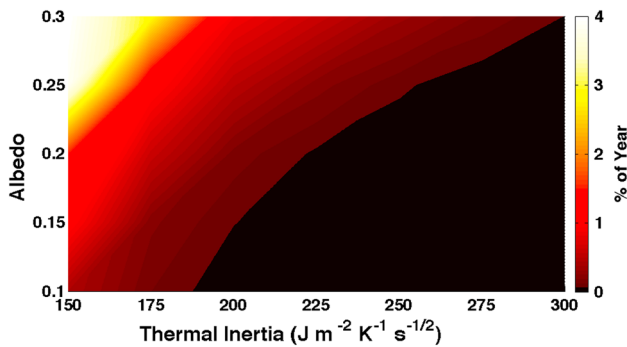


Figure 4. The total percent of the year calcium perchlorate solutions may be possible within the subsurface (down to 1 m) at Gale crater as a function of thermal inertia and albedo. In the color map, 0% is shown as black and values > 4% are white. Color map shading is interpolated between studied cases.

deliquescence of calcium perchlorate is possible in the top few centimeters of the regolith between Ls 100° and 110° for up to 1 hr/sol for the case in Figure 3a ($\Gamma = 180 \text{ J m}^{-2} \text{ K}^{-1} \text{ s}^{-1/2}$, $A = 0.11$). The rover was in this terrain unit between sols 1222 and 1242 or Ls $\sim 94^\circ - 104^\circ$ (Vasavada et al., 2017). For all higher thermal inertia terrains in Figure 3, brine formation is not favored in the subsurface.

To further analyze the potential for liquid formation at Gale crater, we tested combinations of thermal parameters as inferred in the first 1300 sols of the MSL mission (Vasavada et al., 2017). Such simulations can inform on future MSL operation strategies and generally elucidate the potential for liquid formation through deliquescence in equatorial regions on Mars. Simulations were run from $150 \leq \Gamma \leq 300 \text{ J m}^{-2} \text{ K}^{-1} \text{ s}^{-1/2}$ in increments of $\Gamma = 25 \text{ J m}^{-2} \text{ K}^{-1} \text{ s}^{-1/2}$ and for albedo from $0.1 \leq A \leq 0.3$ in increments of $A = 0.05$. In Figure 4, we plot the thermal property parameter space along with the percent of the Martian year brines are possible, which is found as the sum of potential liquid hours over the explored depth compared

to the total hours in a martian year. Simulations suggest that subsurface liquid formation through deliquescence of calcium perchlorate is not favored for terrains where $\Gamma > 300 \text{ J m}^{-2} \text{ K}^{-1} \text{ s}^{-1/2}$. On the other hand, for $\Gamma \lesssim 300 \text{ J m}^{-2} \text{ K}^{-1} \text{ s}^{-1/2}$ liquid formation is possible depending on the albedo while for $\Gamma \lesssim 185 \text{ J m}^{-2} \text{ K}^{-1} \text{ s}^{-1/2}$ liquid formation is possible for a broad range of albedo values. Furthermore, results suggest that conditions are the most apt for brine formation at low thermal inertia ($\Gamma \lesssim 175 \text{ J m}^{-2} \text{ K}^{-1} \text{ s}^{-1/2}$) and high albedo ($A \gtrsim 0.25$) terrains, where brines may be available for up to $\sim 4\%$ of the year; however, such thermal inertia and albedo combinations have not been inferred at Gale crater by MSL through sol 1337 (Vasavada et al., 2017). Most of the studied thermal inertia and albedo combinations inhibit subsurface brine formation, either entirely or limit it to a small fraction of the year.

When brines are possible in the subsurface, the ambient conditions would permit a solution with a water activity of up to $a_w \sim 0.55$, assuming equilibrium where $a_w = (RH_f/100)$. The temperature during the presence of brines is at most $T \sim 205 \text{ K}$. Although potential brines could meet the water activity criteria for Uncertain Regions (Rummel et al., 2014), which requires $a_w \geq 0.5$, it does not simultaneously meet the temperature requirement of $T \geq 250 \text{ K}$. Moreover, at these conditions the composition of the brine would be $\text{Ca}(\text{ClO}_4)_2 = 52.4 \text{ wt\%}$ and $\text{H}_2\text{O} = 47.6 \text{ wt\%}$. Following reported perchlorate concentrations at Gale crater (Leshin et al., 2013) of 0.5 wt% of $\text{Ca}(\text{ClO}_4)_2$ and assuming that all the salt in the regolith were to deliquesce, the resulting solution would be $\sim 0.5 \text{ wt\%}$ water, resulting in a liquid abundance in the regolith of $\sim 1 \text{ wt\%}$ brine. We note that this is an upper limit as it assumes that all the salt deliquesces and the atmosphere can provide sufficient water vapor. Therefore, even when liquids are potentially available in the subsurface, they are only present in small amounts.

4. Discussion and Conclusions

Liquid production through deliquescence has been suggested to be constrained to a few regions on Mars (Kossacki & Markiewicz, 2014; Martínez & Renno, 2013). Therefore, the potential signature of a fair amount of favorable conditions for liquid production at the surface of Gale crater (Martin-Torres et al., 2015), a near-equatorial location, could have implied a more global role for deliquescence. However, here we demonstrate that REMS-derived surface environmental conditions in the first 1648 sols are not favorable to the formation of liquids through deliquescence of calcium perchlorate, which has the lowest known eutectic temperature for single component Mars-relevant brines. Accounting for error in the REMS data, this remains true at the 1-sigma level, but not at the 2-sigma level, where at two times the surface environmental conditions may have permitted liquid formation for up to an hour each day. These points occurred in active sand dunes on sols 1232 and 1311. Derived enthalpic changes may support liquid formation on sol 1232 but not necessarily sol 1311. Generally, though, derived enthalpic changes support the formation of frost at the surface of Gale crater as suggested by Martínez et al. (2016). As such, our results imply that surface liquid formation at Gale crater during MSL's traverse in the first 1648 sols was unlikely.

Simulations of the subsurface environment at Gale crater for the terrains crossed by MSL, though, would suggest that low thermal inertia units could have been occasionally favorable to brine production through

deliquescence in the shallow subsurface for a limited time between Ls 100° and 110°. Therefore, simulations would support the formation of liquids on sol 1232 but in the shallow subsurface; however, they do not support liquid formation on sol 1311 as that is outside the predicted Ls range. Significant inferred enthalpic values (i.e., statistically nonzero) also typically occurred around Ls 100°. Thus, these values may have indicated potential brine formation in the shallow subsurface as well.

A full study of the combination of thermal parameters (i.e., thermal inertia and albedo) suggests that brines may form in terrains with thermal inertia $\Gamma \lesssim 300 \text{ J m}^{-2} \text{ K}^{-1} \text{ s}^{-1/2}$, depending on albedo, and may form for $\Gamma \lesssim 185 \text{ J m}^{-2} \text{ K}^{-1} \text{ s}^{-1/2}$ for a broad range of albedo values. Subsurface brine formation, though, is most favorable in terrains with $\Gamma \lesssim 175 \text{ J m}^{-2} \text{ K}^{-1} \text{ s}^{-1/2}$ and high albedo ($A \gtrsim 0.25$). This could support the potential liquid involvement in Martian slope streaks, which are found in dusty equatorial regions characterized by low thermal inertia (Bhardwaj et al., 2017). The suggested combination of thermal properties required for significant production of subsurface liquids, though, has not yet been traversed by MSL through sol 1337 (Vasavada et al., 2017). However, should the rover encounter such terrain in the future, our results could inform operational strategies for REMS and MSL's Dynamic Albedo of Neutrons instrument, which is used to measure water-equivalent hydrogen in the subsurface (Mitrofanov et al., 2012).

Potential subsurface brines would have water activities of up to $a_w \sim 0.55$ and experience temperatures at most of $T \sim 205 \text{ K}$. As such, these liquids would not be considered habitable to life as we know it nor simultaneously meet the temperature and water activity requirements for Special or Uncertain Regions (Rummel et al., 2014). Assuming typical perchlorate salt concentrations in the Martian regolith and that all the salt enters solution, brine abundance in the regolith is also expected to be low, up to $\sim 1 \text{ wt}\%$, assuming that the atmosphere can supply the water vapor. At these amounts, liquids formed by deliquescence of $\text{Ca}(\text{ClO}_4)_2$ may not support sediment transport but could act as a trigger mechanism to instigate flow. In fact, recent experimental results suggest that grain levitation through vapor released by subsurface liquids may reduce the amount of fluid needed to form flow behavior by nearly an order of magnitude (Raack et al., 2017). Furthermore, though recent models propose a granular flow mechanism for RSL formation, a trigger mechanism for flow initiation is still required, a potential role for liquids (Dundas et al., 2017).

Our results suggest that only under a restricted set of conditions can calcium perchlorate solutions form at Gale crater, Mars; however, we only considered a single-salt brine system and simulated conditions on flat terrain. The Martian regolith, though, is a mixture of various salts (e.g., Hecht et al. (2009), Hanley et al. (2012), and Elsenousy et al. (2015)). Brines with multiple dissolved salts may have lower eutectic temperatures and deliquescence relative humidities and thus be more stable under present-day Martian conditions (Gough et al., 2014). Therefore, once deliquescence is permitted in the subsurface of low thermal inertia terrains within Gale crater, dissolution may form multisalt brines that would have increased stability relative to pure component solutions. Furthermore, slope effects on thermal insolation and horizontal distribution of water vapor will also affect the formation of brines. Indeed, as water vapor is transported across Gale crater, it is reduced due to surface-atmosphere interactions at the crater walls (Steele et al., 2017). Consequently, the walls of Gale crater may provide more apt conditions to the formation of liquids through deliquescence.

Simulations on the formation of subsurface brines at Gale crater suggest that the search for liquids on present-day Mars by MSL may be most successful in the shallow subsurface of terrains characterized by low thermal inertia and high albedo and specifically around Ls 100°. Furthermore, using Gale crater as a proxy for equatorial regions on Mars, we suggest that humidity-temperature conditions are typically inconsistent with deliquescence in such regions. At most, the sum of the time the humidity-temperature conditions permit for deliquescence of calcium perchlorate in the subsurface (down to 1 m) is 4%. Terrains that may meet the required thermal properties ($\Gamma \lesssim 185 \text{ J m}^{-2} \text{ K}^{-1} \text{ s}^{-1/2}$ for a broad range of albedos) to favor deliquescence account for only about half of the equatorial region on Mars (Mellon et al., 2000). Even in these terrains, only small amounts of liquids would be expected to form. Therefore, in equatorial regions, though deliquescence may play a role in triggering mass wasting events, such as potentially in RSL formation (Dundas et al., 2017), it is unlikely to be a dominant atmosphere-regolith water vapor exchange process in contrast with polar regions, such as the Phoenix landing site, where deliquescence is expected to play a more active role in the near-surface exchange of water vapor (Nuding et al., 2014).

Acknowledgments

This material is based upon work supported by the National Aeronautics and Space Administration (NASA) under grant NNX15AM42G issued through the Mars Data Analysis Program. R. V. Gough acknowledges support from the NASA MSL Participating Scientist Program. K. M. Primm acknowledges support from NASA's Earth and Space Science Fellowship grant NNX15AT60H. M. Tolbert acknowledges support from NASA's Mars Fundamental Research program through grant NNX14AJ96G. G. M. Martinez acknowledges support from the Jet Propulsion Laboratory through grant 1449038. All Mars Science Laboratory Rover Environmental Monitoring Station data used in this work are publicly available on the NASA Planetary Data System, Planetary Atmospheres Node. Data supporting Figures 2, 3, and 4 are provided in the supporting information. The authors thank the anonymous reviewers for valuable comments that helped improve this manuscript.

References

- Aharonson, O., & Schorghofer, N. (2006). Subsurface ice on Mars with rough topography. *Journal of Geophysical Research*, *111*, E11007. <https://doi.org/10.1029/2005JE002636>
- Applebaum, J., & Flood, D. J. (1989). *Solar radiation on Mars* (pp. 1–34). Cleveland, OH: NASA Technical Memorandum.
- Bhardwaj, A., Sam, L., Martin-Torres, F. J., Zorzano, M.-P., & Fonseca, R. M. (2017). Martian slope streaks as plausible indicators of transient water activity. *Science Reports*, *7*, 7074.
- Blackburn, D. G., Bryson, K., Chevrier, V. F., & Roe, L. A. (2009). Sublimation kinetics of CO₂ ice on Mars. *Planetary and Space Science*, *58*, 780–791.
- Brass, G. W. (1980). Stability of brines on Mars. *Icarus*, *42*(1), 20–28.
- Bryson, K. L., Chevrier, V. F., Sears, D. W. G., & Ulrich, R. (2008). Stability of ice on Mars and the water vapor diurnal cycle: Experimental study of the sublimation of ice through a fine-grained basaltic regolith. *Icarus*, *196*, 446–458.
- Chevrier, V., Sears, D., Chittenden, J., Roe, L., Ulrich, R., Bryson, K., et al. (2007). Sublimation rate of ice under simulated Mars conditions and the effect of layers of mock regolith JSC Mars-1. *Geophysical Research Letters*, *34*, L02203. <https://doi.org/10.1029/2006GL028401>
- Chevrier, V. F., & Altheide, T. S. (2008). Low temperature aqueous ferric sulfate solutions on the surface of Mars. *Geophysical Research Letters*, *35*, L22101. <https://doi.org/10.1029/2008GL035489>
- Chevrier, V. F., & Rivera-Valentin, E. G. (2012). Formation of recurring slope lineae by liquid brines on present-day Mars. *Geophysical Research Letters*, *39*, L21202. <https://doi.org/10.1029/2012GL054119>
- Chevrier, V. F., Hanley, J., & Altheide, T. S. (2009). Stability of perchlorate hydrates and their liquid solutions at the Phoenix landing site, Mars. *Geophysical Research Letters*, *36*, L10202. <https://doi.org/10.1029/2009GL037497>
- Christensen, P. R., Bandfield, J. L., Hamilton, V. E., Ruff, S. W., Kieffer, H. H., Titus, T. N., et al. (2001). Mars Global Surveyor Thermal Emission Spectrometer experiment: Investigation description and surface science results. *Journal of Geophysical Research*, *106*, 23,823–23,871.
- Clark, B. C. (1978). Implications of abundant hygroscopic minerals in the Martian regolith. *Icarus*, *34*(3), 645–665.
- Clifford, S. M., & Hillel, D. (1986). Knudsen diffusion—The effect of small pore size and low gas pressure on gaseous transport in soil. *Soil Science*, *141*, 289–297.
- Cull, S. C., Arvidson, R. E., Catalano, J. G., Ming, D. W., Morris, R. V., Mellon, M. T., & Lemmon, M. (2010). Concentrated perchlorate at the Mars Phoenix landing site: Evidence for thin film liquid water on Mars. *Geophysical Research Letters*, *37*, L22203. <https://doi.org/10.1029/2010GL045269>
- Dundas, C. M., McEwen, A. S., Chojnacki, M., Milazzo, M. P., Byrne, S., McElwaine, J. N., & Urso, A. (2017). Granular flows at recurring slope lineae on Mars indicate a limited role for liquid water. *Nature Geoscience*, *10*, 903–907.
- Elsensouy, A., Hanley, J., & Chevrier, V. F. (2015). Effect of evaporation and freezing on the salt paragenesis and habitability of brines at the Phoenix landing site. *Earth and Planetary Science Letters*, *421*, 39–46.
- Feistel, R., & Wagner, W. (2007). Sublimation pressure and sublimation enthalpy of H₂O ice Ih between 0 and 273.16K. *Geochimica et Cosmochimica Acta*, *71*(1), 36–45.
- Fischer, E., Martinez, G. M., Elliott, H. M., & Renno, N. O. (2014). Experimental evidence for the formation of liquid saline water on Mars. *Geophysical Research Letters*, *41*, 4456–4462. <https://doi.org/10.1002/2014GL060302>
- Fischer, E., Martinez, G. M., & Renno, N. O. (2016). Formation and Persistence of Brine on Mars: Experimental simulations throughout the diurnal cycle at the Phoenix landing site. *Astrobiology*, *16*(12), 937–948.
- Glavin, D. P., Freissinet, C., & Miller, K. E. (2013). Evidence for perchlorates and the origin of chlorinated hydrocarbons detected by SAM at the Rocknest aeolian deposit in Gale Crater. *Journal of Geophysical Research: Planets*, *118*, 1955–1973. <https://doi.org/10.1002/jgre.20144>
- Gomez-Elvira, J., Armiens, C., Castañer, L., Domínguez, M., Genzer, M., Gómez, F., et al. (2012). REMS: The environmental sensor suite for the Mars science laboratory rover. *Space Science Reviews*, *170*(1–4), 583–640.
- Gough, R. V., Chevrier, V. F., & Tolbert, M. A. (2014). Formation of aqueous solutions on Mars via deliquescence of chloride-perchlorate binary mixtures. *Earth and Planetary Science Letters*, *393*, 73–82.
- Gough, R. V., Chevrier, V. F., & Tolbert, M. A. (2016). Formation of liquid water at low temperatures via the deliquescence of calcium chloride: Implications for Antarctica and Mars. *Planetary and Space Science*, *131*, 79–87.
- Gough, R. V., Chevrier, V. F., Baustian, K. J., Wise, M. E., & Tolbert, M. A. (2011). Laboratory studies of perchlorate phase transitions: Support for metastable aqueous perchlorate solutions on Mars. *Earth and Planetary Science Letters*, *312*(3–4), 371–377.
- Grotzinger, J. P., Crisp, J., Vasavada, A. R., Anderson, R. C., Baker, C. J., Barry, R., et al. (2012). Mars science laboratory mission and science investigation. *Space Science Reviews*, *170*, 5–56.
- Haberle, R. M., McKay, C. P., Schaeffer, J., Cabrol, N. A., Grin, E. A., Zent, A. P., & Quinn, R. (2001). On the possibility of liquid water on present-day Mars. *Journal of Geophysical Research*, *106*(E10), 23,317–23,326.
- Hamilton, V. E., Vasavada, A. R., Sebastián, E., de la Torre Juárez, M., Ramos, M., Armiens, C., et al. (2014). Observations and preliminary science results from the first 100 sols of MSL Rover Environmental Monitoring Station ground temperature sensor measurements at Gale Crater. *Journal of Geophysical Research: Planets*, *119*, 745–770. <https://doi.org/10.1002/2013JE004520>
- Hanley, J., Chevrier, V. F., Berget, D. J., & Adams, R. D. (2012). Chlorate salts and solutions on Mars. *Geophysical Research Letters*, *39*, L08201. <https://doi.org/10.1029/2012GL051239>
- Harri, A. M., Genzer, M., & Kemppinen, O. (2014). Mars Science Laboratory relative humidity observations: Initial results. *Journal of Geophysical Research: Planets*, *119*, 2132–2147. <https://doi.org/10.1002/2013JE004514>
- Hecht, M. H., Kounaves, S. P., Quinn, R. C., West, S. J., Young, S. M. M., Ming, D. W., et al. (2009). Detection of perchlorate and the soluble chemistry of Martian soil at the Phoenix lander site. *Science*, *325*, 64–67.
- Hudson, O., Aharonson, T. L., Schorghofer, N., Farmer, C., Hecht, M., & Bridges, N. (2007). Water vapor diffusion in Mars subsurface environments. *Journal of Geophysical Research*, *112*, E05016. <https://doi.org/10.1029/2006JE002815>
- Hudson, T. L., & Aharonson, O. (2008). Diffusion barriers at Mars surface conditions: Salt crusts, particle size mixtures, and dust. *Journal of Geophysical Research*, *113*, E09008. <https://doi.org/10.1029/2007JE003026>
- Ingersoll, A. P. (1970). Mars: Occurrence of liquid water. *Science*, *168*(3934), 972–973.
- Jensen, E. J., Diskin, G., Lawson, R. P., Lance, S., Paul Bui, T., Hilavka, D., et al. (2013). Ice nucleation and dehydration in the Tropical Tropopause Layer. *Proceedings of the National Academy of Sciences*, *110*, 2041–2046.
- Jia, X., Gu, W., Li, Y. J., Cheng, P., Tang, Y., Guo, L., et al. (2018). Phase transitions and hygroscopic growth of Mg(ClO₄)₂, NaClO₄, and NaClO₄·H₂O: Implications for the stability of aqueous water in hyperarid environments on Mars and on Earth. *ACS Earth and Space Chemistry*, *2*, 159–167.
- Johnsson, A., Reiss, D., Hauber, E., Hiesinger, H., & Zanetti, M. (2014). Evidence for very recent melt-water and debris flow activity in gullies in a young mid-latitude crater on Mars. *Icarus*, *235*, 37–54.

- Kereszturi, A., & Rivera-Valentín, E. G. (2012). Locations of thin liquid water layers on present-day Mars. *Icarus*, 221(1), 289–295.
- Kereszturi, A., Möhlmann, D., Berczi, S., Ganti, T., Horvath, A., Kuti, A., et al. (2010). Indications of brine related local seepage phenomena on the northern hemisphere of Mars. *Icarus*, 207, 149–164.
- Kossacki, K. J., & Markiewicz, W. J. (2014). Seasonal flows on dark Martian slopes, thermal condition for liquescence of salts. *Icarus*, 233, 126–130.
- Kreslavsky, M. A., & Head, J. W. (2009). Slope streaks on Mars: A new wet mechanism. *Icarus*, 201(2), 517–527.
- Leshin, L. A., Mahaffy, P. R., Webster, C. R., Cabane, M., Coll, P., Conrad, P. G., et al. (2013). Volatile, isotope, and organic analysis of Martian fines with the Mars curiosity rover. *Science*, 341(6153), 123,8937–123,8937.
- Malin, M., & Edgett, K. (2003). Evidence for persistent flow and aqueous sedimentation on early Mars. *Science*, 302, 1931–1934.
- Maltagliati, L., Montmessin, F., Fedorova, A., Korabiev, O., Forget, F., & Bertaux, J. L. (2011). Evidence of water vapor in excess of saturation in the atmosphere of Mars. *Science*, 333(6051), 1868–1871.
- Marion, G. M., Catling, D. C., Zahnle, K. J., & Claire, M. W. (2010). Modeling aqueous perchlorate chemistries with applications to Mars. *Icarus*, 207(2), 675–685.
- Martin-Torres, F. J., Zorzano, M.-P., Valentin-Serrano, P., Harri, A.-M., Genzer, M., Kempainen, O., et al. (2015). Transient liquid water and water activity at Gale crater on Mars. *Nature Geoscience*, 8(5), 357–361.
- Martínez, G. M., & Renno, N. O. (2013). Water and brines on Mars: Current evidence and implications for MSL. *Space Science Reviews*, 175(1–4), 29–51.
- Martínez, G. M., Fischer, E., Renno, N. O., Sebastián, E., Kempainen, O., Bridges, N., et al. (2016). Likely frost events at Gale crater: Analysis from MSL/REMS measurements. *Icarus*, 280, 93–102.
- Martínez, G. M., Newman, C. N., De Vicente-Retortillo, A., Fischer, E., Renno, N. O., Richardson, M. I., et al. (2017). The modern near-surface Martian climate: A review of in-situ meteorological data from viking to curiosity. *Space Science Reviews*, 105(17), 6222–44.
- Martínez, G. M., Renno, N., Fischer, E., Borlina, C. S., Hallet, B., Torre Juárez, M., et al. (2014). Surface energy budget and thermal inertia at Gale Crater: Calculations from ground-based measurements. *Journal of Geophysical Research: Planets*, 119, 1822–1838. <https://doi.org/10.1002/2014JE004618>
- Massé, M., Conway, S. J., Gargani, J., Patel, M. R., Pasquon, K., McEwen, A., et al. (2016). Transport processes induced by metastable boiling water under Martian surface conditions. *Nature Geoscience*, 9, 425–428.
- McEwen, A., Dundas, C. M., Mattson, S. S., Toigo, A. D., Ojha, L., Wray, J. J., et al. (2013). Recurring slope lineae in equatorial regions of Mars. *Nature Geoscience*, 7, 53–58.
- McEwen, A., Ojha, L., Dundas, C. M., Mattson, S. S., Byrne, S., Wray, J. J., et al. (2011). Seasonal flows on warm Martian slopes. *Science*, 333, 740–743.
- Mellon, M. T., Jakosky, B. M., Kieffer, H. H., & Christensen, P. R. (2000). High-resolution thermal inertia mapping from the Mars Global Surveyor Thermal Emission Spectrometer. *Icarus*, 148, 437–455.
- Ming, D. W., Archer, P. D., Glavin, D. P., Eigenbrode, J. L., Franz, H. B., Sutter, B., et al. (2014). Volatile and organic compositions of sedimentary rocks in Yellowknife Bay, Gale Crater, Mars. *Science*, 343(6169), 1245267.
- Mitrofanov, I. G., Litvak, M. L., Varenikov, A. B., Barmakov, Y. N., Behar, A., Bobrovniksky, Y. I., et al. (2012). Dynamic Albedo of Neutrons (DAN) Experiment Onboard NASA Mars Science Laboratory. *Space Science Reviews*, 170, 559–582.
- Murphy, D. M., & Koop, T. (2005). Review of the vapour pressures of ice and supercooled water for atmospheric applications. *Quarterly Journal of the Royal Meteorological Society*, 131(608), 1539–1565.
- Navarro-Gonzalez, R., Vargas, E., de la Rosa, J., Raga, A. C., & McKay, C. P. (2010). Reanalysis of the Viking results suggests perchlorate and organics at midlatitudes on Mars. *Journal of Geophysical Research*, 115, E12010. <https://doi.org/10.1029/2010JE003599>
- Nikolalakos, G., & Whiteway, J. A. (2017). Laboratory study of adsorption and deliquescence on the surface of Mars. *Icarus*, 308, 221–229. <https://doi.org/10.1016/j.icarus.2017.05.006>
- Nuding, D. L., Gough, R. V., Venkateswaran, K. J., Spry, J. A., & Tolbert, M. A. (2017). Laboratory investigations on the survival of Bacillus subtilis spores in deliquescent salt Mars analog environments. *Astrobiology*, 17, 997–1008.
- Nuding, D. L., Rivera-Valentín, E. G., Davis, R. D., Gough, R. V., Chevrier, V. F., & Tolbert, M. A. (2014). Deliquescence and efflorescence of calcium perchlorate: An investigation of stable aqueous solutions relevant to Mars. *Icarus*, 243, 420–428.
- Ojha, L., Wilhelm, M. B., Murchie, S. L., McEwen, A. S., Wray, J. J., Hanley, J., et al. (2015). Spectral evidence for hydrated salts in recurring slope lineae on Mars. *Nature Geoscience*, 8, 829–832.
- Pal, B., & Kereszturi, A. (2017). Possibility of microscopic liquid water formation at landing sites on Mars and their observational potential. *Icarus*, 282, 84–92.
- Pestova, O. N., Myund, L. A., Khripun, M. K., & Prigaro, A. V. (2005). Polythermal study of the systems $M(ClO_4)_2 \cdot H_2O$. *Russian Journal of Applied Chemistry*, 78(3), 409–413.
- Pollack, J. B., Haberle, R. M., & Murphy, J. R. (1990). Simulations of the general circulation of the Martian atmosphere 2. Seasonal pressure variations. *Journal of Geophysical Research*, 98, 3149–3181.
- Putzig, N. E., Mellon, M. T., Kretke, K. A., & Arvidson, R. E. (2005). Global thermal inertia and surface properties of Mars from the MGS mapping mission. *Icarus*, 173(2), 325–341.
- Raack, J., Conway, S. J., Hery, C., Balme, M. R., Carpy, S., & Patel, M. R. (2017). Water induced sediment levitation enhances downslope transport on Mars. *Nature Communications*, 8, 1151.
- Rapp, D. (2008). *Human missions to Mars: Enabling technologies for exploring the Red Planet*. New York: Springer.
- Rennó, N. O., Bos, B. J., Catling, D., Clark, B. C., Drube, L., Fisher, D., et al. (2009). Possible physical and thermodynamical evidence for liquid water at the Phoenix landing site. *Journal of Geophysical Research*, 114, E00E03. <https://doi.org/10.1029/2009JE003362>
- Rivera-Valentín, E. G., Blackburn, D. G., & Ulrich, R. (2011). Revisiting the thermal inertia of Iapetus: Clues to the thickness of the dark material. *Icarus*, 216, 347–358.
- Rivera-Valentín, E. G., & Chevrier, V. F. (2015). Revisiting the Phoenix TECP data: Implications for regolith control of near-surface humidity on Mars. *Icarus*, 253, 156–158.
- Rodríguez Colon, B., & Rivera-Valentín, E. G. (2016). Investigating the biological potential of Gale crater's subsurface. *LPSC XLVII*, 2026.
- Rummel, J. D., Beaty, D. W., Jones, M. A., Bakermans, C., Barlow, N. G., Boston, P. J., et al. (2014). A new analysis of Mars special regions: Findings of the second MEPAG Special regions science analysis group (SR-SAG2). *Astrobiology*, 14(11), 887–968.
- Savijärvi, H., Harri, A.-M., & Kempainen, O. (2016). The diurnal water cycle at Curiosity: Role of exchange with the regolith. *Icarus*, 265, 63–69.
- Schmidt, F., Douté, S., Schmitt, B., Vincendon, M., Bibring, J.-P., Langevin, Y., & The Omega Team (2009). Albedo control of seasonal South Polar cap recession on Mars. *Icarus*, 200(2), 374–394.
- Schorghofer, N., & Aharonson, O. (2005). Stability and exchange of subsurface ice on Mars. *Journal of Geophysical Research*, 110, E54413. <https://doi.org/10.1029/2004JE002350>

- Sebastián, E., Armiens, C., Gómez-Elvira, J., Zorzano, M. P., Martínez-Frias, J., Esteban, B., & Ramos, M. (2010). The rover environmental monitoring station ground temperature sensor: A pyrometer for measuring ground temperature on Mars. *Sensors*, *10*, 9211–9231.
- Sizemore, H. G., & Mellon, M. T. (2008). Laboratory characterization of the structural properties controlling dynamical gas transport in Mars-analog soils. *Icarus*, *197*, 606–620.
- Steele, L. J., Balme, M. R., Lewis, S. R., & Spiga, A. (2017). The water cycle and regolith-atmosphere interaction at Gale crater, Mars. *Icarus*, *289*, 56–79.
- Stillman, D. E., & Grimm, R. E. (2011). Dielectric signatures of adsorbed and salty liquid water at the Phoenix landing site, Mars. *Journal of Geophysical Research*, *116*, E09005. <https://doi.org/10.1029/2011JE003838>
- Sullivan, R. E., Thomas, P., Veverka, J., Malin, M., & Edgett, K. S. (2001). Mass movement slope streaks imaged by the Mars Orbiter Camera. *Journal of Geophysical Research*, *106*, 23,607–23,633.
- Ulrich, R. (2009). Modeling diffusion advection in the mass transfer of water vapor through Martian regolith. *Icarus*, *201*, 127–134.
- Vasavada, A. R., Piqueux, S., Lewis, K. W., Lemmon, M. T., & Smith, M. D. (2017). Thermophysical properties along Curiosity's traverse in Gale crater, Mars, derived from REMS ground temperature sensor. *Icarus*, *284*, 372–386.
- York, D., Evensen, N. M., López Martínez, M., & De Basabe Delgado, J. (2004). Unified equations for the slope, intercept, and standard errors of the best straight line. *American Journal of Physics*, *72*, 367–375.
- Zent, A. P., Haberle, R. M., Houben, H. C., & Jakosky, B. M. (1993). A coupled subsurface-boundary layer model of water on Mars. *Journal of Geophysical Research*, *98*, 3319–3337.
- Zent, A. P., Hecht, M. H., Cobos, D. R., Wood, S. E., Hudson, T. L., Milkovich, S. M., et al. (2010). Initial results from the thermal and electrical conductivity probe (TECP) on Phoenix. *Journal of Geophysical Research*, *115*, E00E14. <https://doi.org/10.1029/2009JE003420>
- Zorzano, M. P., Mateo-Martí, E., Prieto-Ballesteros, O., Osuna, S., & Renno, N. (2009). Stability of liquid saline water on present day Mars. *Geophysical Research Letters*, *36*, L20201. <https://doi.org/10.1029/2009GL040315>